Supplementary Information (SI) for Journal of Materials Chemistry B.

Screening of an antimicrobial peptide-TWPAL and its application in hydrogels for wound healing

Huinan Wang[a], Fengyuan Gao[b], Muhammad Rafiq[b], Bing Yu[a*], Qinghai Niu[d], Hailin Cong[c*]

a. School of Chemistry and Chemical Engineering, Qingdao University, Qingdao, 266071, China

b. School of Materials Science and Engineering, Shandong University of Technology, Zibo 255000, China

c. School of Materials Science and Engineering, Shandong University of Technology, Zibo 255000, China

d. Linyi Kangli Medical Devices Co., Ltd., Linyi, China

*Corresponding authors at: School of Chemistry and Chemical Engineering, Qingdao University, Qingdao, 266071, China

E-mail addresses: yubing198@qdu.edu.cn (B. Yu); conghailin@sdut.edu.cn (H. Cong)

Figure S1. SEM image of (a) SiO_2 microspheres; (b) E. coli-encapsulated SiO_2 microspheres; (c) S. aureus-encapsulated SiO_2 microspheres. (d) FT-IR spectra of SiO2 microspheres, SiO_2 microspheres grafted with DR, SiO_2 -DR-EC, and SiO_2-DR-SA; (e) TGA curves of SiO_2 micro-spheres, SiO_2 -DR-EC, and SiO_2-DR-SA.

Figure S2. Characterization before and after DR illumination.

Figure S3. (a) Adsorption of antimicrobial peptides by S. aureus membrane chromatography microspheres; (b) Adsorption of antimicrobial peptides by E. coil membrane microspheres.

Figure S4. Circular dichroism (CD) spectrum of TWPAL.

Figure S5. Potential diagram of H_2O, TWPAL, E. coli, S. aureus, E. coli membrane, S. aureus membrane.

Figure S6. FTIR of hydrogel.

Figure S7. In vitro antibacterial test of TWPAL and TWPAL-gel, against E. coli and S. aureus.

Figure S8. MIC of TWPAL-gel against E. coli and S. aureus.

Figure S9. Tensile stress–strain curve of hydrogel.

Figure S10. Shear strength of hydrogel.

Figure S11. Stability of antimicrobial peptide TWPAL: (a) The stability of TWPAL in different pH; (b) The stability of TWPAL in NaOH solution (PH=12); (c) The stability of TWPAL in artificial gastric juiuice (pH=2); (d) The stability of TWPAL in different temperature; (e) The stability of TWPAL in different concentrations of H_2O_2; (f) The stability of TWPAL in different concentrations of NaCl.

Figure S12. Drug resistance test of antimicrobial peptide hydrogel TWPAL-gel: (a) Photos of LB plate for TWPAL-gel resistance test; (b) TWPAL-gel and gentamycin sulfate MIC curve of S. aureus; (c) TWPAL-gel and gentamycin sulfate MIC curve of E. coli.

Figure S13.Wound area statistics of different groups.

Figure S14. Body weight change rate of mice in each group.

Table 1. The adsorption results of different peptides on different microspheres.

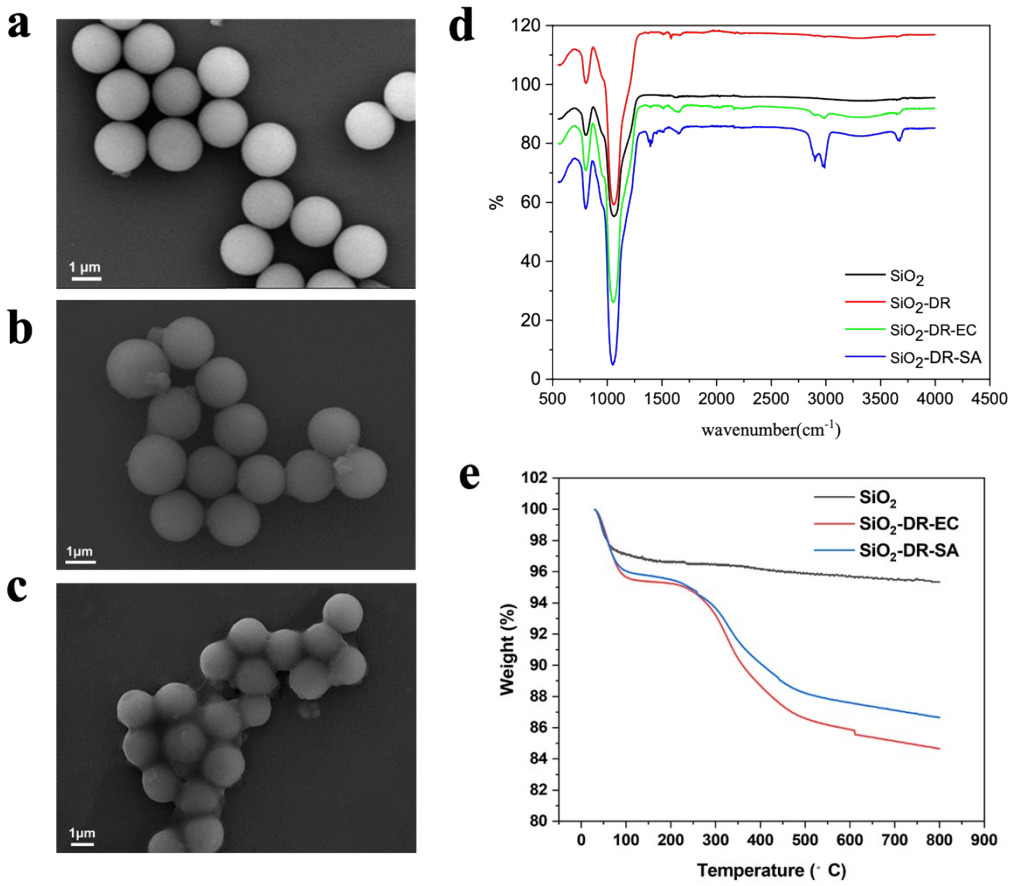

Figure S1. SEM image of (a) SiO_2 microspheres; (b) E. coli-encapsulated SiO_2 microspheres; (c) S. aureus-encapsulated SiO_2 microspheres. (d) FT-IR spectra of SiO_2 microspheres, SiO_2 microspheres grafted with DR, SiO_2 -DR-EC, and SiO_2-DR-SA; (e) TGA curves of SiO_2 micro-spheres, SiO_2 -DR-EC, and SiO2-DR-SA.

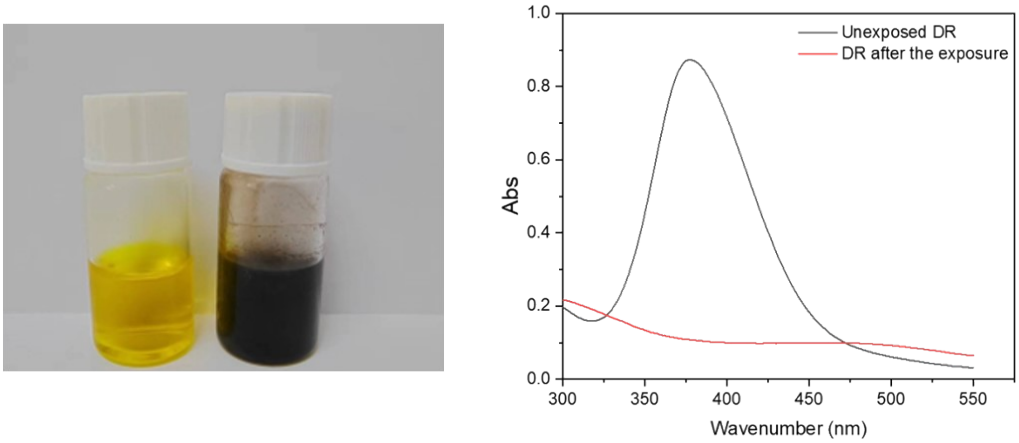

Figure S2. Characterization before and after DR illumination.

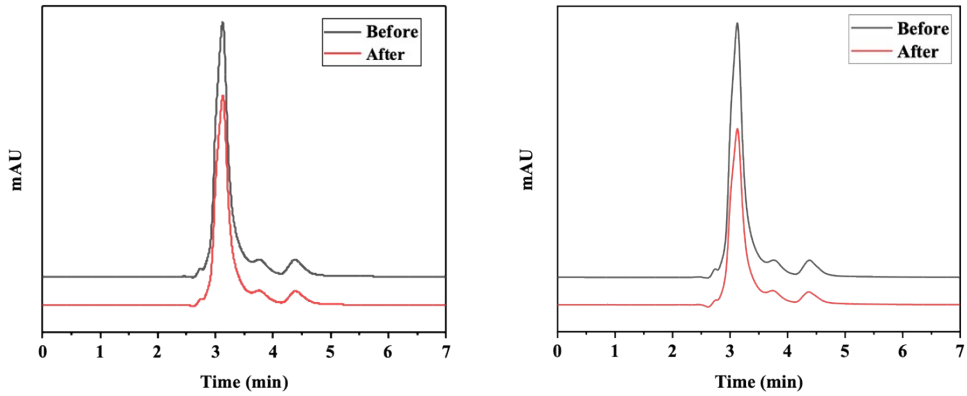

Figure S3. (a) Adsorption of antimicrobial peptides by S. aureus membrane chromatography microspheres; (b) Adsorption of antimicrobial peptides by E. coil membrane microspheres.

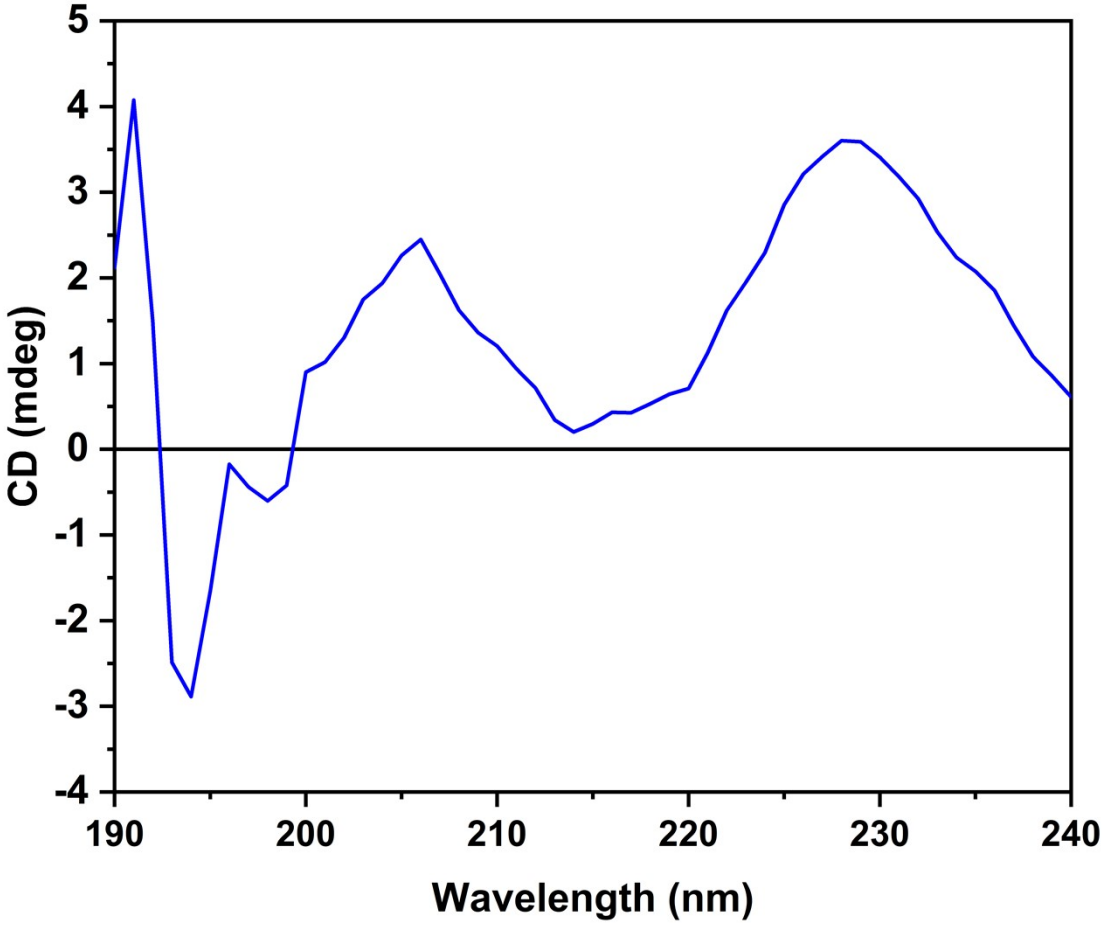

Figure S4. Circular dichroism (CD) spectrum of TWPAL.

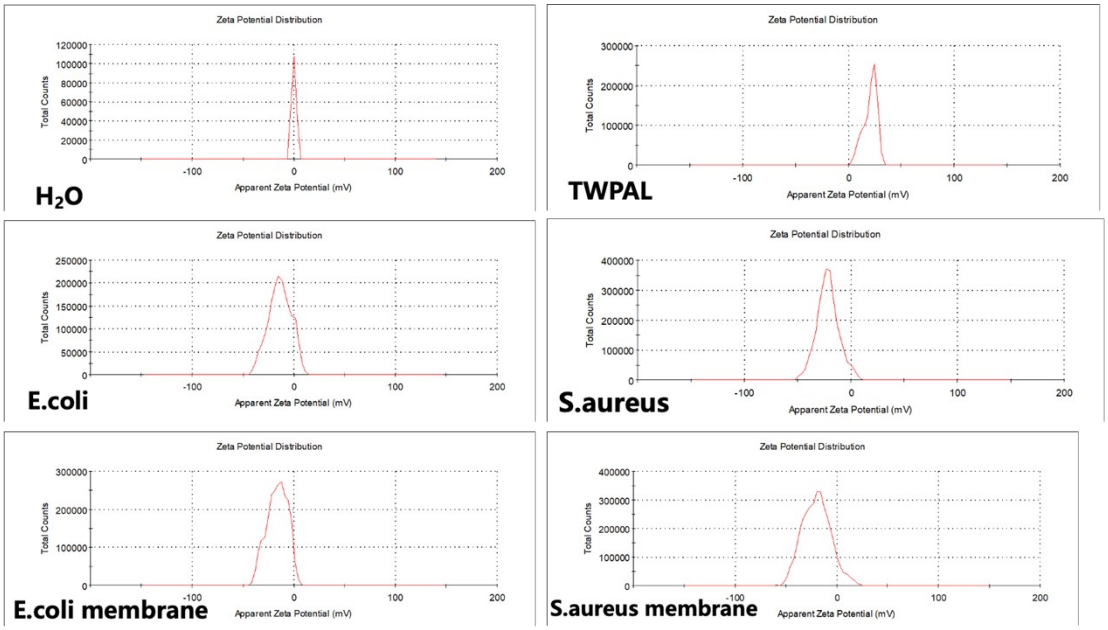

Figure S5. Potential diagram of H_2O, TWPAL, E. coli, S. aureus, E. coli membrane, S. aureus membrane.

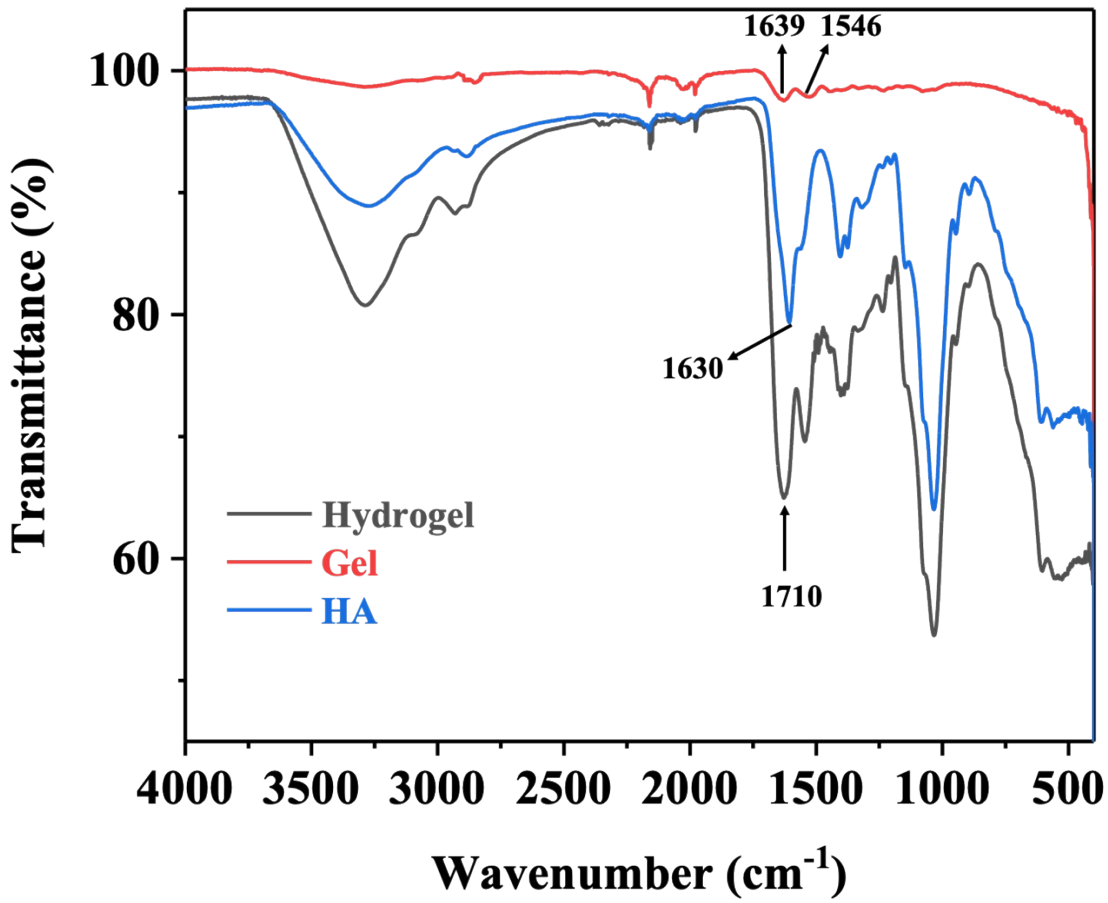

Figure S6. FTIR of hydrogel.

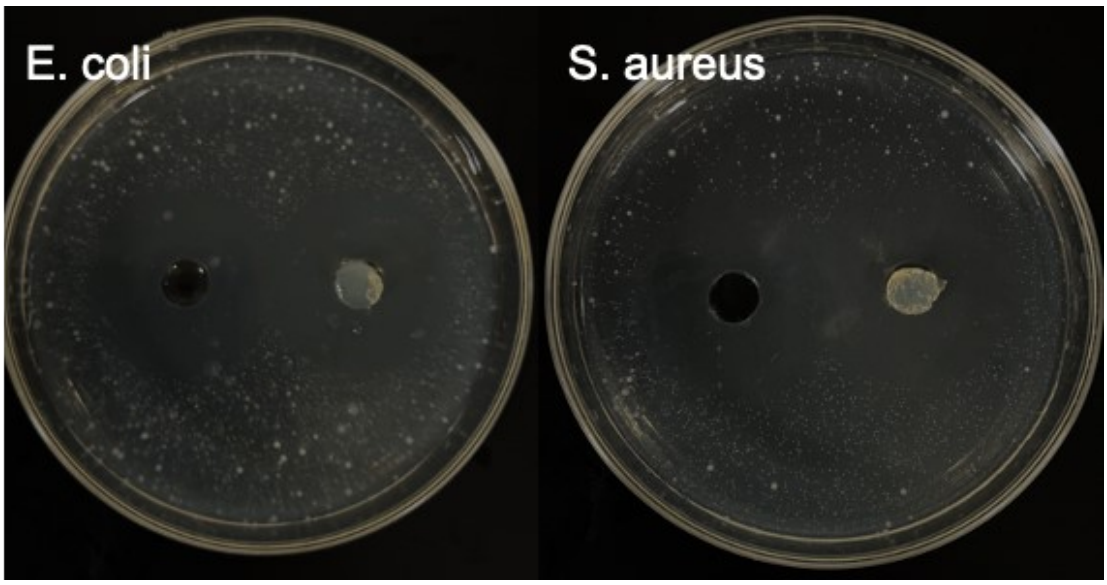

Figure S7. In vitro antibacterial test of TWPAL and TWPAL-gel, against E. coli and S. aureus.

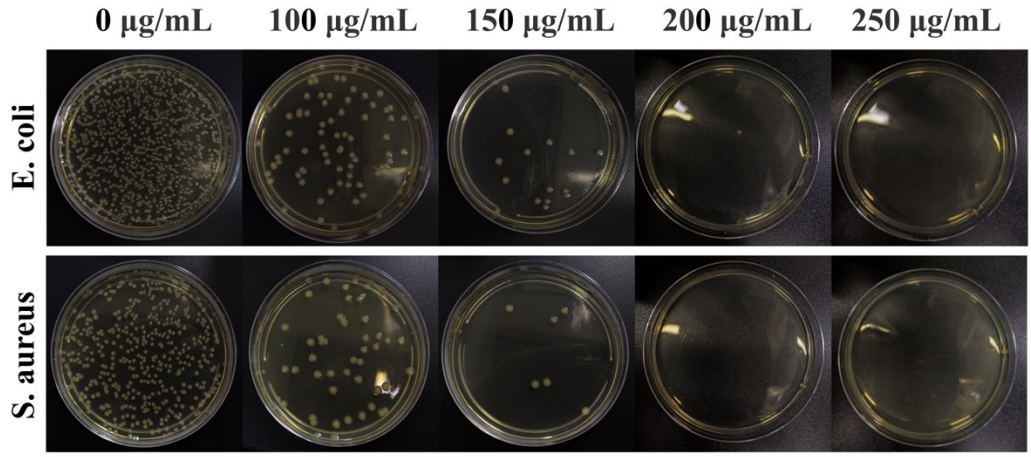

Figure S8. MIC of TWPAL-gel against E. coli and S. aureus.

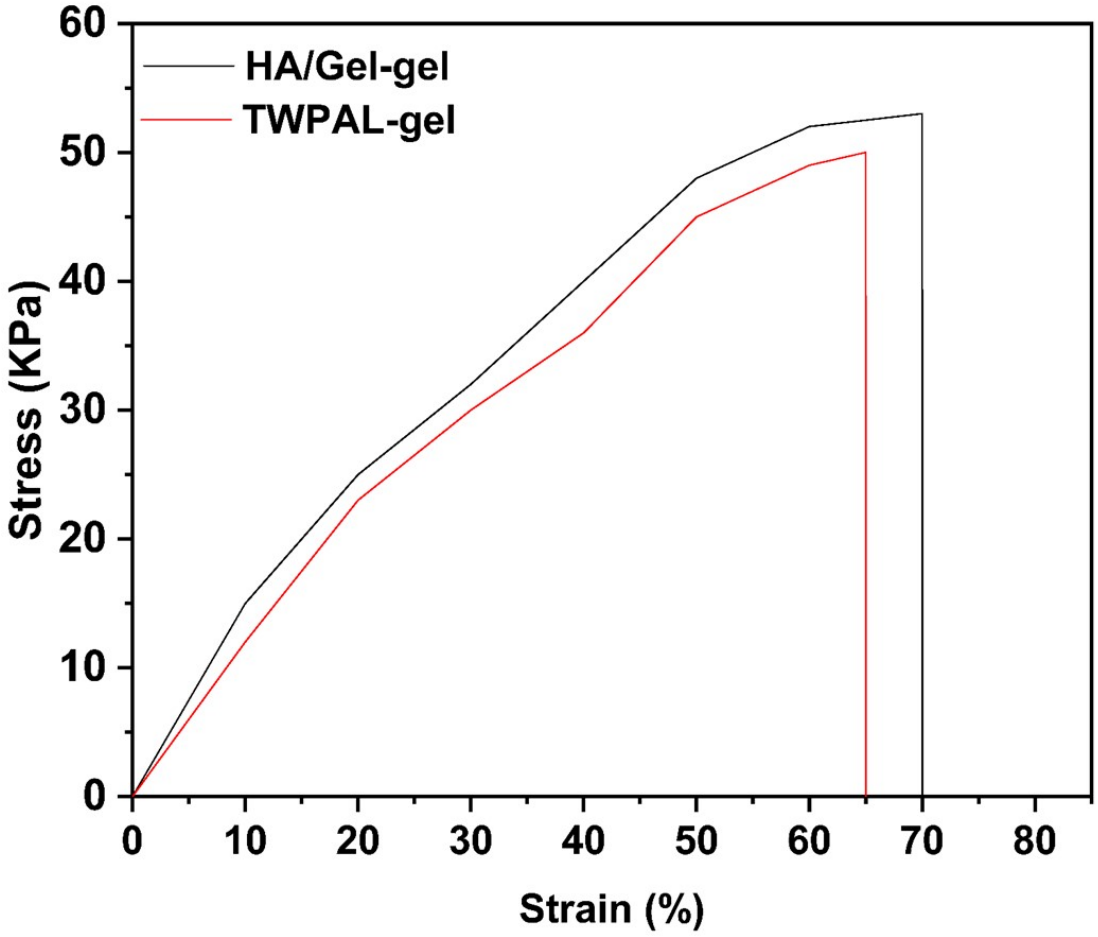

Figure S9. Tensile stress–strain curve of hydrogel.

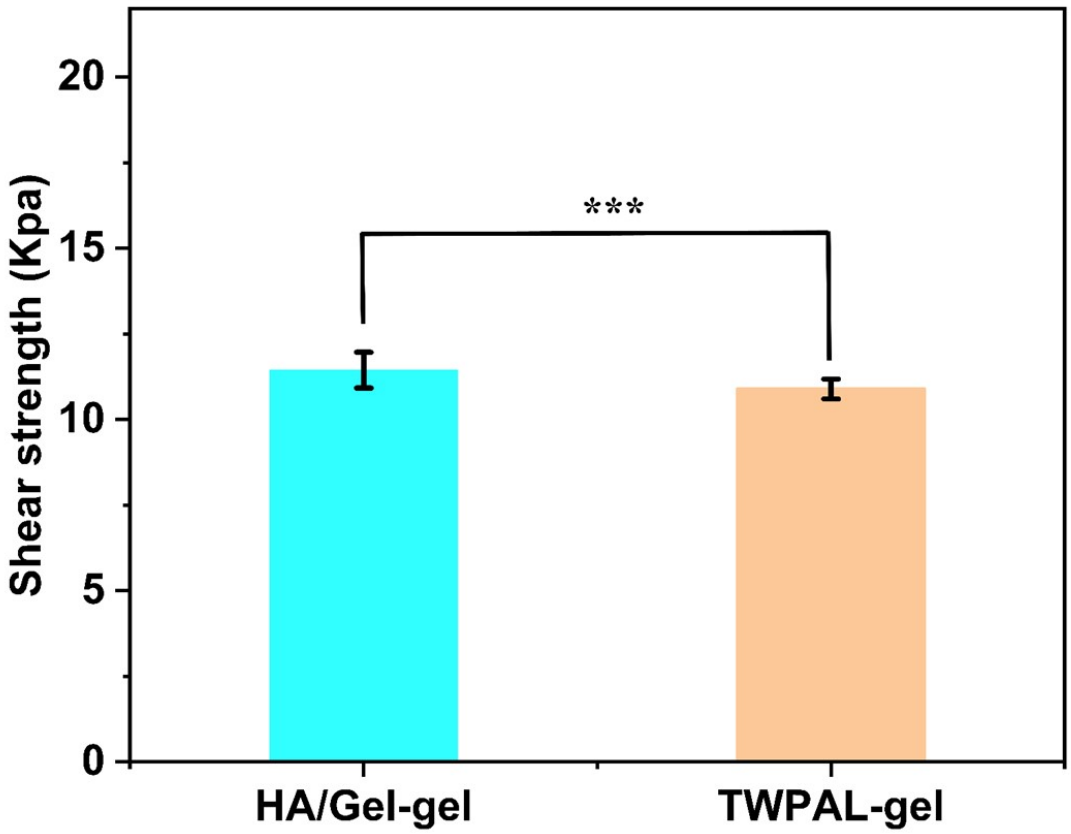

Figure S10. Shear strength of hydrogel.

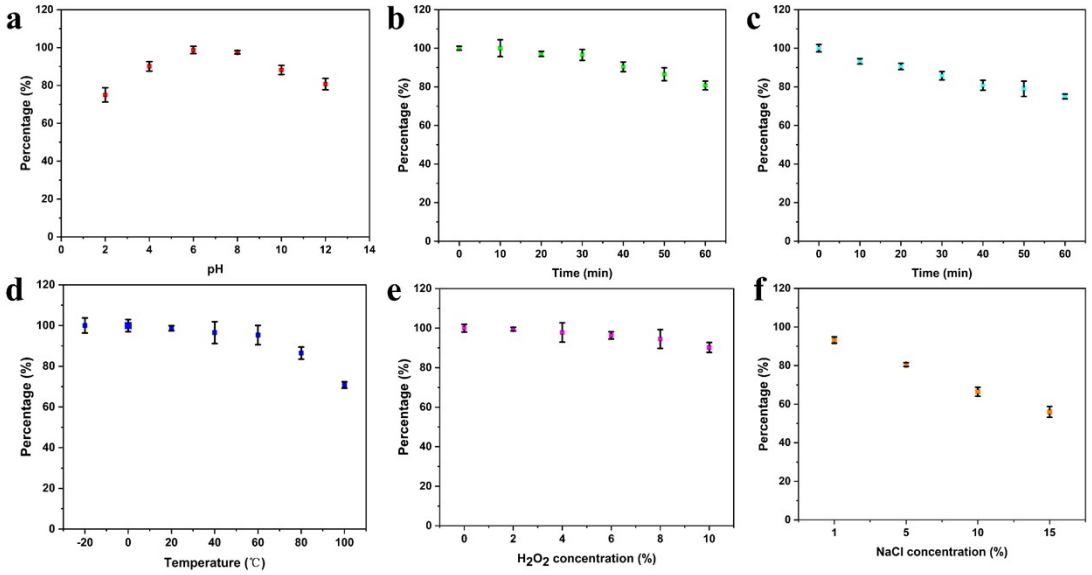

Figure S11. Stability of antimicrobial peptide TWPAL: (a) The stability of TWPAL in different pH; (b) The stability of TWPAL in NaOH solution (PH=12); (c) The stability of TWPAL in artificial gastric juiuice (pH=2); (d) The stability of TWPAL in different temperature; (e) The stability of TWPAL in different concentrations of H_2O_2; (f) The stability of TWPAL in different concentrations of NaCl.

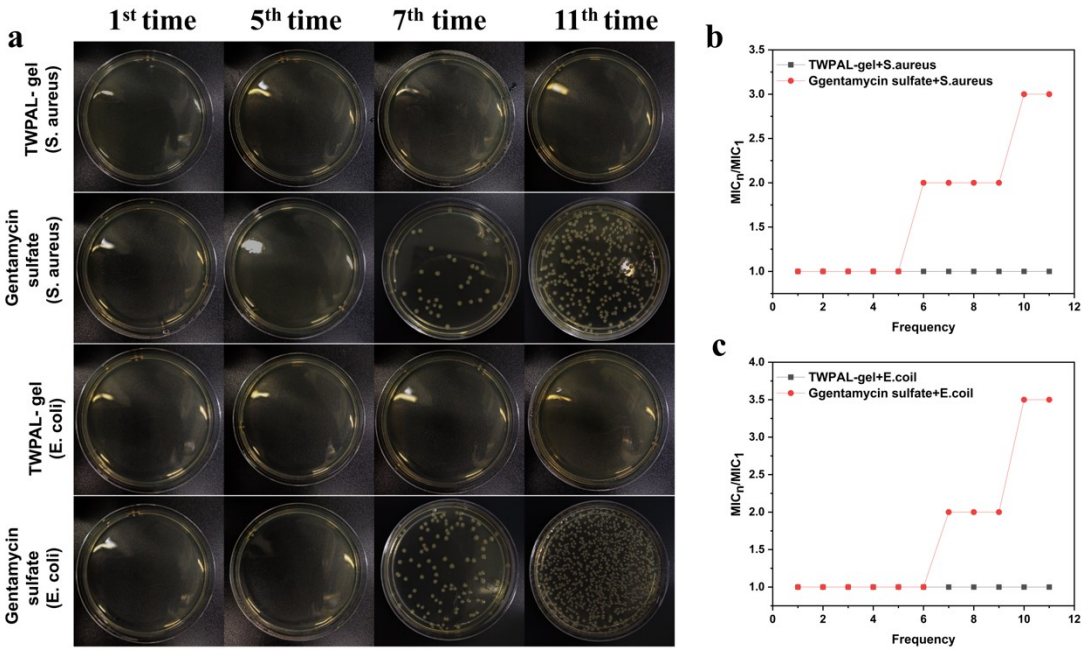

Figure S12. Drug resistance test of antimicrobial peptide hydrogel TWPAL-gel: (a) Photos of LB plate for TWPAL-gel resistance test; (b) TWPAL-gel and gentamycin sulfate MIC curve of S. aureus; (c) TWPAL-gel and gentamycin sulfate MIC curve of E. coli.

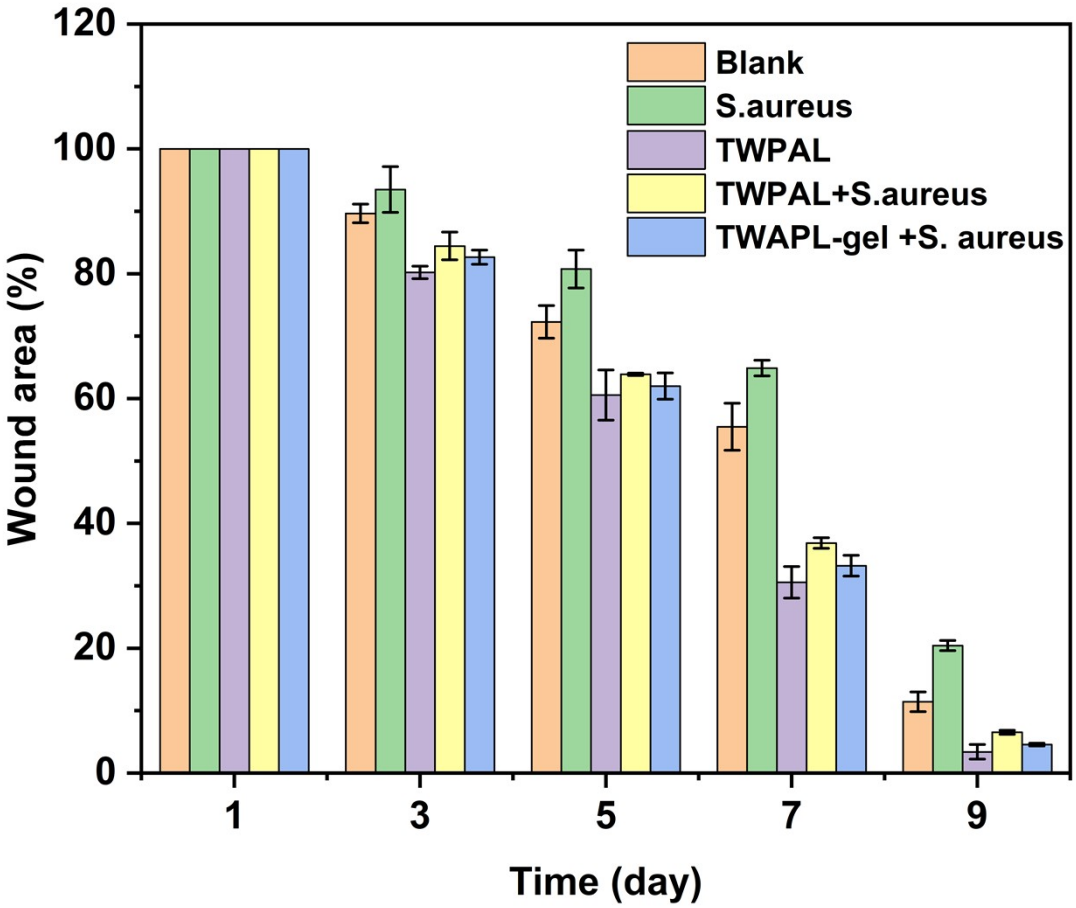

Figure S13.Wound area statistics of different groups.

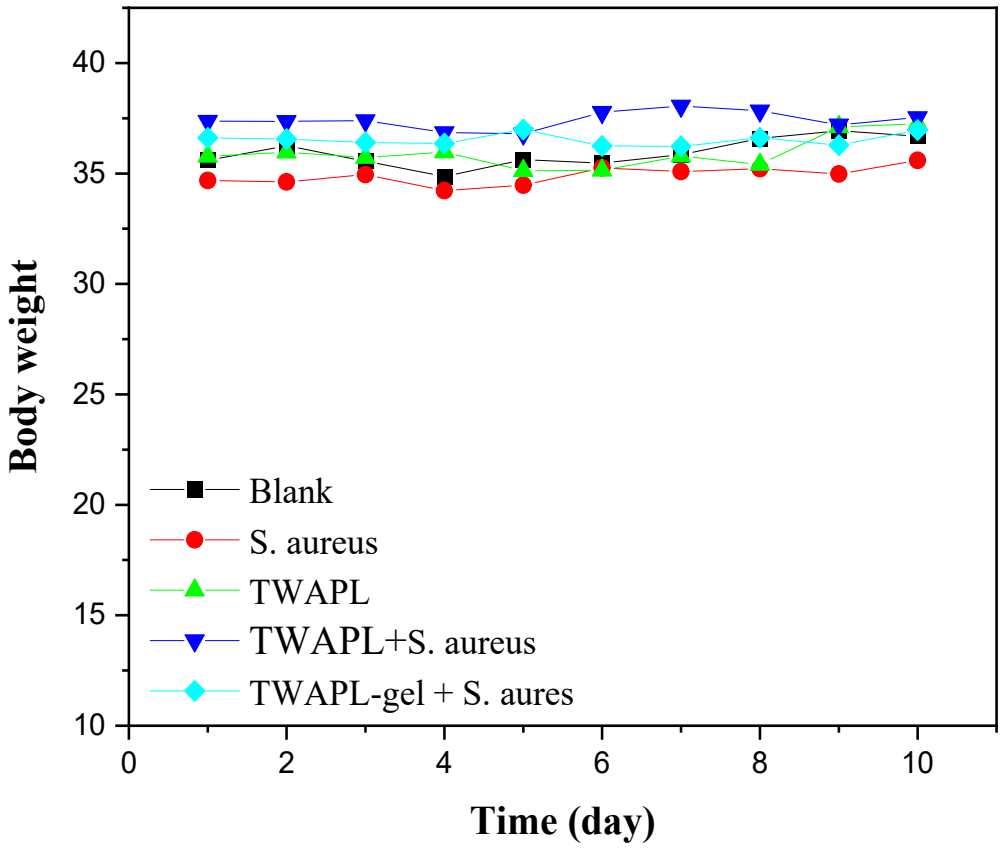

Figure S14. Body weight change rate of mice in each group.

Table S1. The adsorption results of different peptides on different microspheres

The serial number	Types of peptides	Peak area change ratio (%)		
		Blank	*E. coli*	*S. aureus*
1	TWGAF	10.2685	9.4997	10.5827
2	TWPAF	8.7320	10.6143	13.8019
3	TWPAL	11.3501	21.4430	23.9171
4	TWGAL	9.4246	8.2452	9.0542